

Forsterite Powder Prepared from Water-Soluble Hybrid Precursor

N. I. Maliavski, O. V. Dushkin, J. V. Markina, and G. Scarinci

Dept. of General Chemistry, Moscow University of Civil Engineering, 129337 Moscow, Russia

Partially polycondensed γ -aminopropylsilanetriol (APSTOL) was used as the silica precursor to prepare magnesium orthosilicate in the form of crystalline forsterite. Aqueous solutions of APSTOL and magnesium acetate were mixed and dried forming a water-soluble product that was converted into forsterite by heating to 1,000°C. The thermal evolution of the system was studied using TGA, FTIR, UV-VIS spectrophotometry, and XRD techniques, especially for the acetate decomposition and transformation of CSiO_3 -tetrahedra into the orthosilicate anions. The combustion of organics and the crystallization of forsterite proceed at temperatures 350 and 870°C, respectively. At intermediate temperatures, the system contains amorphous silicates with oligomeric and polymeric anions, which gradually depolymerize as temperature increases. The resulting crystalline product contains less impurities (periclase and enstatite) than samples prepared using other wet-chemistry techniques.

Introduction

Ceramics of the forsterite (Mg_2SiO_4) composition are widely applied in bulk, thin film, and powder forms, mainly because of the excellent electrical and thermal insulating properties. Apart from traditional high-temperature methods, sol-gel techniques also were applied to prepare forsterite powders and films starting from tetraethoxysilane (TEOS) and magnesium alkoxides dissolved in ethanol (Saiki and Kanai, 1985; Burlich et al., 1991).

Recently, we proposed a new wet-chemistry method to prepare high-basicity silicates, including forsterite, based on the use of partially polycondensed γ -aminopropylsilanetriol (APSTOL) as the silica precursor (Maliavski et al., 1997). APSTOL can be easily synthesized from γ -aminopropyltriethoxysilane (APTEOS), and is highly soluble in water and stable in aqueous solutions practically at any pH value. That creates important advantages for this precursor in comparison with another type of water-soluble silica precursor, aminosilicates (Maliavski and Guglielmi, 1988). These are stable only at $\text{pH} \geq 11$ that usually complicates the synthesis of high-basicity silicates, as well as any silicates of Mg, Ca, Ti, Zr, Bi, Fe and other metals not forming either stable cation complexes or water-soluble or amphoteric hydroxides.

In the present study, we focused on the synthesis of polycrystalline forsterite starting from aqueous solutions of APSTOL and various magnesium salts to choose the optimum precursor mixture and process parameters. Another purpose was to follow the thermal evolution of the system considering the three main processes: the formation of silicate structures from the precursor mixtures, the depolymerization of silicate anions, and the crystallization of forsterite.

Experimental Studies

Sample preparation

APSTOL solution was prepared by mixing APTEOS (Aldrich, 98%) with water at the molar ratio $\text{H}_2\text{O}/\text{APTEOS} = 8.0$, and by stirring the mixture for 15–30 min to complete the hydrolysis process. The resulted clear solution with $\text{pH} = 11.3$ contained 18.9% of silica and was used as the silica precursor. The carbonization extent due to the reaction of NH_2 group with CO_2 , was evaluated by measuring the volume of CO_2 escaped after acidifying the solution, and the molar ratio $\text{HCO}_3^-/\text{NH}_2$ was found to be 0.015.

To obtain the binary precursor, the aqueous solution (30 wt. %) of a magnesium salt (acetate, nitrate or sulfate) was mixed with the APSTOL solution at a molar ratio $\text{MgO}/\text{SiO}_2 = 2$. Then, the corresponding acid (50 wt. % aqueous solu-

Correspondence concerning this article should be addressed to N. I. Maliavski.
Current address of G. Scarinci: Dipartimento di Ingegneria Meccanica, Università di Padova, via Venezia, 1, 35131 Padova, Italy.

tion of CH_3COOH , HNO_3 or H_2SO_4) was added to bring the solution pH to 4 to prevent the precipitation of $\text{Mg}(\text{OH})_2$. If magnesium basic carbonate was used as the MgO precursor, the binary precursor was prepared in the form of a suspension of $[\text{Mg}(\text{OH})_2]\text{CO}_3$ in the APSTOL solution.

After drying the prepared solutions in air at 125°C for 24 h, green gels were obtained. These gels were then grinded and finally dried in a desiccator for several days resulting in powdered dry gels soluble in water (excluding the magnesium basic carbonate case). As a reference, two samples were prepared according to the traditional sol-gel scheme, starting from TEOS and magnesium salts (acetate and nitrate) dissolved in ethanol. Unlike the APSTOL-based solutions which gelled only after dehydration, the gelation of TEOS-based ones occurred after heating at 75°C for 5 h in closed containers. Then, dry gels were prepared as described.

The crystalline products were obtained by heating the dry gels up to $1,000^\circ\text{C}$ at $5^\circ\text{C}/\text{min}$. In the case of the $\text{Mg}(\text{NO}_3)_2$ -APSTOL system, the heat treatment was performed only up to 400°C . There was a highly exothermic red-ox reaction which began between amino-groups and nitrate anions, and resulted in a polyphase crystalline product.

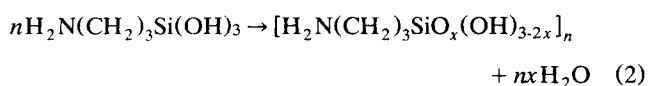
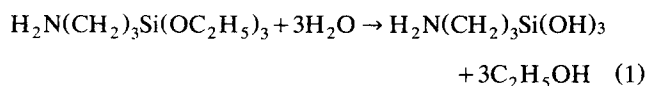
Sample characterization

Thermogravimetric analysis (TGA) and differential thermal analysis (DTA) were run to $1,000^\circ\text{C}$ at a heating rate $5^\circ\text{C}/\text{min}$ using a Paulik-Paulik-Erdey apparatus (Q-1000) with a multiplate platinum holder. Powder X-ray diffraction (XRD) was performed by a JEOL diffractometer (JDX-10PA) using $\text{Cu K}\alpha$ radiation. Phase concentrations were evaluated by calculating the main peaks areas using pure minerals as standards. Infrared spectra of thin films deposited on silicon wafers were measured at 400 – $4,000\text{ cm}^{-1}$ by Fourier transform infrared (FTIR) spectroscopy using a Perkin Elmer 2000 apparatus.

The polymeric structure of silicate anions in the samples was studied quantitatively using continuous UV-VIS spectrophotometry ($\lambda = 410\text{ nm}$) of the reaction between molybdic acid and an acid solution of the sample (Iler, 1979; Maliavski et al., 1994). The latter was prepared by adding one part of the milled sample to 200 parts of 0.15N HCl and stirring the mixture for 1 h at 5°C (Maliavski et al., 1985).

Results and Discussion

The interaction between APTEOS and water involves both hydrolysis and condensation steps and can be given by two reactions



According to previous investigations, the solid APSTOL films dried at room temperature contain oligomer species together with a polymer network (Wang and Jones, 1993). After being dried at 200°C , the structure of APSTOL is probably close to

a partially cross-linked linear polymer with a notable concentration of silanols (Maliavski et al., 1997). In solutions and green gels, the magnesium salts presumably do not react with the aminosiloxane oligomers and polymers or significantly affect connectivity of their structure. This explains the good solubility of gels in water.

Thermogravimetry and differential thermal analysis

Figure 1 shows TGA and DTA curves for the green gel prepared from APSTOL and magnesium acetate, in comparison with those for the magnesium salt alone.

(1) Thermal decomposition of the orthosilicate gel can be separated in three principal stages in the 100 – 250°C , 370 – 600°C , and 870 – 930°C temperature ranges.

(2) The first stage is due to the escape of hydrate and silanol water and is coherent with the DTA endotherm at 140°C . The similar endotherms were observed also for magnesium acetate (Figure 1b) (see Gardner and Messing, 1984) and APSTOL (Maliavski et al., 1997).

(3) The second stage consists of two steps accompanied with DTA exotherms at 400°C and 570°C , and a broad intermediate zone with a regular mass loss. It is very intensive (the total mass loss is near 50%) and includes the oxidative decomposition of both precursors. The decomposition temperatures of pure magnesium acetate and APSTOL are 380°C and 420°C , respectively, but in the present case, the corresponding stages cannot be separated. The exotherm at 570°C probably indicates the oxidation of the residual organ-

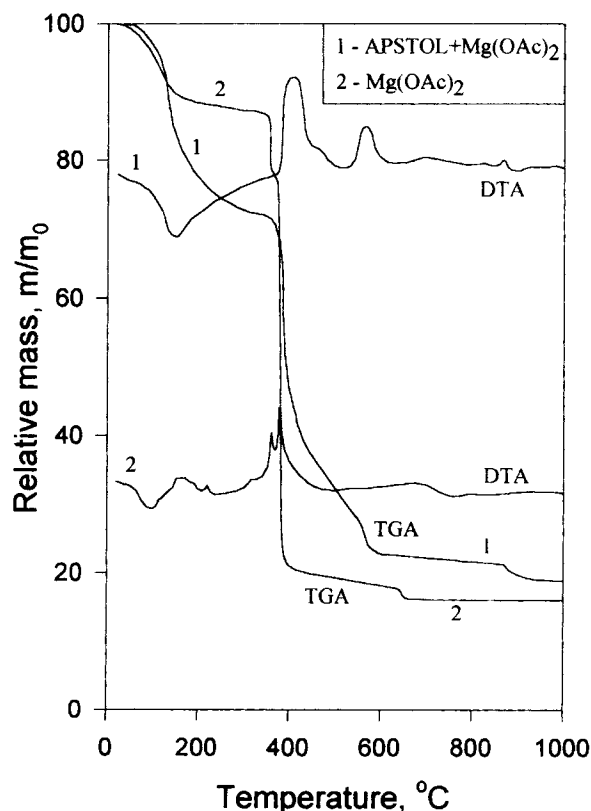


Figure 1. TGA and DTA curves for the forsterite (APSTOL-magnesium acetate system) and magnesium acetate gels, $5^\circ\text{C}/\text{min}$.

Table 1. Crystalline Phases of Samples Fired Up to 1,000°C at a Heating Rate 5°C/min

Precursors of SiO ₂ and MgO	Temperature (°C)		Concentrations (vol. %)			Other Phases
	Decomp.	Cryst.	Forsterite	Periclase	Enstatite	
TEOS + Mg(NO ₃) ₂	480	840	85	8	6	—
TEOS + Mg(OCOCH ₃) ₂	500	890	85	5	8	—
APSTOL + [Mg(OH)] ₂ CO ₃	600	860	65	16	9	—
APSTOL + Mg(NO ₃) ₂	(400)	(400)	40	3	< 1	Tridimite, amorphous phases
APSTOL + MgSO ₄	780	880	43	2	11	MgSO ₄
APSTOL + Mg(OCOCH ₃) ₂	600	870	93	< 1	< 1	—

ics and is generally characteristic for hybrid silica precursors (Murakami et al., 1989).

(4) The third decomposition stage accompanied with a weak exotherm at 870°C is due to forsterite crystallization with simultaneous oxidation of the last carbon residues (the mass loss is 1.8%). The powder, which is dark brown when heated to 800°C, becomes grayish-white after this stage.

Concerning the other prepared gels, the corresponding temperatures of final decomposition and crystallization are displayed in Table 1. The data obtained indicate that crystallization temperatures are almost independent of the precursors used (except for the system APSTOL–magnesium nitrate where the highly exothermic redox reaction occurs at 400°C) and fall within a narrow temperature region 850–890°C. On the contrary, temperatures of the end of the decomposition are generally higher for the APSTOL-based systems than for the TEOS-based ones, because of some delays in the formation of SiO₄ units as a result of the gradual oxidation of Si–C bonds.

X-ray diffraction

All the two-component samples after being heated to 1,000°C (5°C/min) are well crystallized, and the main crystalline phase is orthorhombic forsterite (the principal peak at 36.4° corresponds to $d = 2.46$ Å). For example, Figure 2 shows XRD patterns obtained for two binary samples heated to 1,000°C: APSTOL–Mg(OCOCH₃)₂ (together with the corresponding dry gel and xerogel) and TEOS–Mg(NO₃)₂. Other binary samples show similar patterns, however, indicating the lower forsterite content and higher concentrations of impurities. Two principal types of crystalline impurities are MgO (periclase, the main peak at 42.8°) and MgSiO₃ (enstatite, the main peak at 31°). Other detected phases are SiO₂ (tridimite), MgSO₄, and amorphous phases. The phase concentrations evaluated for binary samples are displayed in Table 1 (as percentages in relation to pure phases).

It is obvious that only three systems are suitable for the preparation of crystalline forsterite: APSTOL–magnesium acetate and both TEOS-based systems. The systems APSTOL–MgSO₄ and APSTOL–Mg(NO₃)₂ are inefficient because of the relatively high thermal stability of MgSO₄ and the explosive redox process at 400°C, respectively. One interesting feature is that for the system APSTOL–magnesium basic carbonate, rather high concentrations of forsterite are also obtained (65% of the maximum one) in spite of insolubility of [Mg(OH)]₂CO₃ and hence the heterogeneity of the system.

However, as shown in Table 1, the best results are obtained for the system APSTOL–Mg(OCOCH₃)₂ that indicates a high chemical homogeneity of the corresponding gels. Such behavior can probably be linked to the well-known knowledge of hard crystallization of concentrated aqueous solutions of magnesium acetate caused by their high viscosity. From the diffractogram of the APSTOL–acetate dry gel (Figure 2a), it can be seen that after heating to 150°C the gel is highly amorphous, without notable amounts of crystalline magnesium acetate. This could explain the low concentration of crystalline MgO in the binary system heated to 600°C that is above decomposition temperature (Figure 2b). Heated to 1,000°C, this system gives pure forsterite with only a small amount of the periclase impurity.

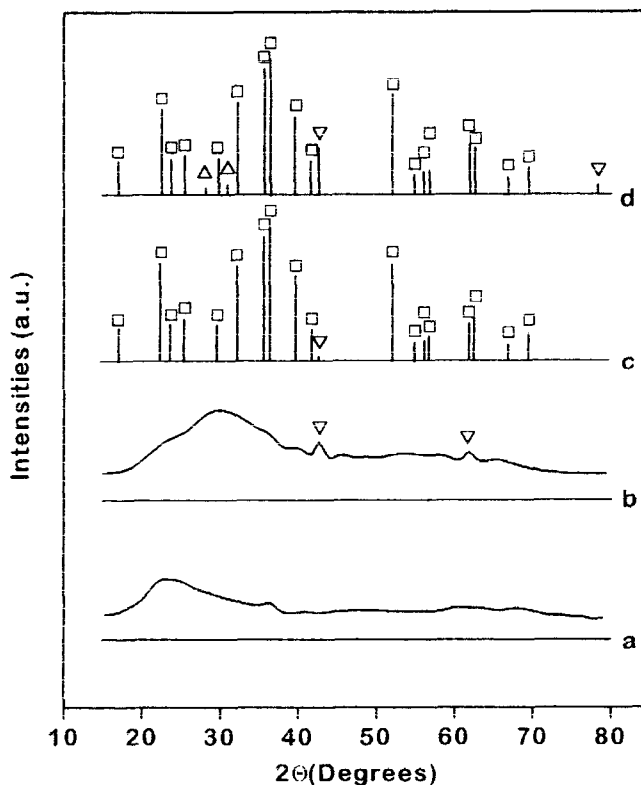


Figure 2. XRD patterns of APSTOL + Mg(OCOCH₃)₂: (a) dry gel; (b) sample heated to 600°C; (c) sample heated to 1,000°C; TEOS + Mg(NO₃)₂; (d) sample treated to 1,000°C.

Crystalline phases: forsterite (squares); periclase (triangles pointing down); enstatite (triangles pointing up).

Gel-to-silicate transition

The thermal evolution of the binary MgO-SiO_2 system after the decomposition of the precursor was studied additionally using FTIR data for the most efficient system APSTOL-magnesium acetate.

Figure 3 shows FTIR spectra (in the characteristic region $400\text{--}2,000\text{ cm}^{-1}$) of the corresponding dry gel films heated at $5^\circ\text{C}/\text{min}$ to five different temperatures. The most evident results of the heat treatment are the following:

(A) At 150°C , the sample presents the pair of bands at $1,010$ and $1,075\text{ cm}^{-1}$ assigned to $\nu\text{ Si-O}$ and characteristic for gels containing trifunctional silicon atoms (Innocenzi et al., 1994). By 400°C , it turns to a single broad peak centered at $1,025\text{ cm}^{-1}$ whose shape is rather typical for amorphous silicates.

(B) At $400\text{--}750^\circ\text{C}$, the position of the peak corresponding to the Si-O stretching vibration, shifts towards lower wavenumbers from $1,025$ to 925 cm^{-1} that should indicate a general trend to the depolymerization of silicate network.

(C) At 950°C , the spectrum is substantially modified: the diffuse peak of $\nu\text{ Si-O}$ turns to a system of rather sharp peaks attributable to crystalline forsterite (Handke and Urban, 1982), with the main peak at 880 cm^{-1} .

(D) Intensities of the peaks attributed to acetate anion (at $1,600$, $1,430$, $1,360$, 660 and 610 cm^{-1}) which are dominant at 150°C , still remain rather high at 400°C . However, they drastically reduce above this temperature (except the region $1,600\text{--}1,700\text{ cm}^{-1}$ where notable absorption remained,

possibly due to adsorbed water and/or organics residuals containing $\text{C}=\text{C}$ bonds).

The obtained FTIR data indicate that at these heating conditions, the oxidative decomposition of magnesium acetate follows that of APSTOL with some delay. This non-coincidence should retard the formation of orthosilicate structures by creating amorphous magnesium-rich phases, for example, amorphous high-basicity silicates or amorphous magnesia, whereas the periclase content is low according to the XRD results. This suggestion is confirmed partially by the presence of a broad absorption band at about 600 cm^{-1} (also observed for acetate derived magnesia by Baraldi, 1982) in the spectra of the samples heated to 550°C and 750°C .

Such an assumption is in good agreement with the results of UV-VIS monitoring that give more direct information on the polymerization state of the samples. In Figure 4, the content of acid-soluble silica (that is, the percentage of SiO_2 which can be extracted with HCl and detected by the molybdate method) and the average basicity of silicate anions are displayed with dependence on temperature. For the present case, the basicity (x) means the molar ratio MgO/SiO_2 in silicates and indicates the polymerization degree of the silicate anions. For example, $x = 2$ for the monomer (orthosilicate), $x = 1.5$ for the dimer, $x = 1.0$ for the wollastonite-like linear polymer and $x = 0$ for pure silica. For the linear oligomers, the basicity is connected with the polymerization degree (n) according to the expression $x = 1 + 1/n$.

The values of acid solubility of silica can reflect the APSTOL-silicate transformation if we consider that trifunc-

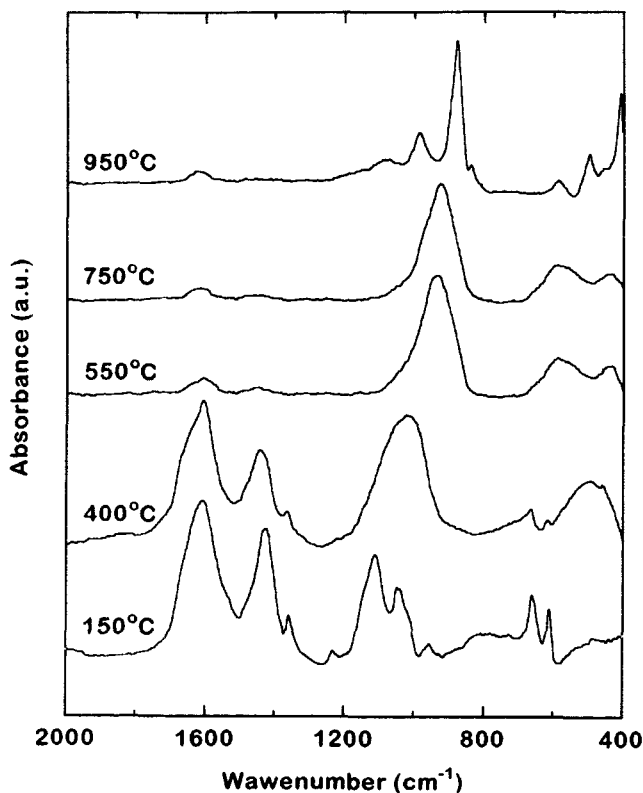


Figure 3. Evolution of FTIR spectra of the forsterite dry gel (APSTOL-magnesium acetate system) heated at $5^\circ\text{C}/\text{min}$.

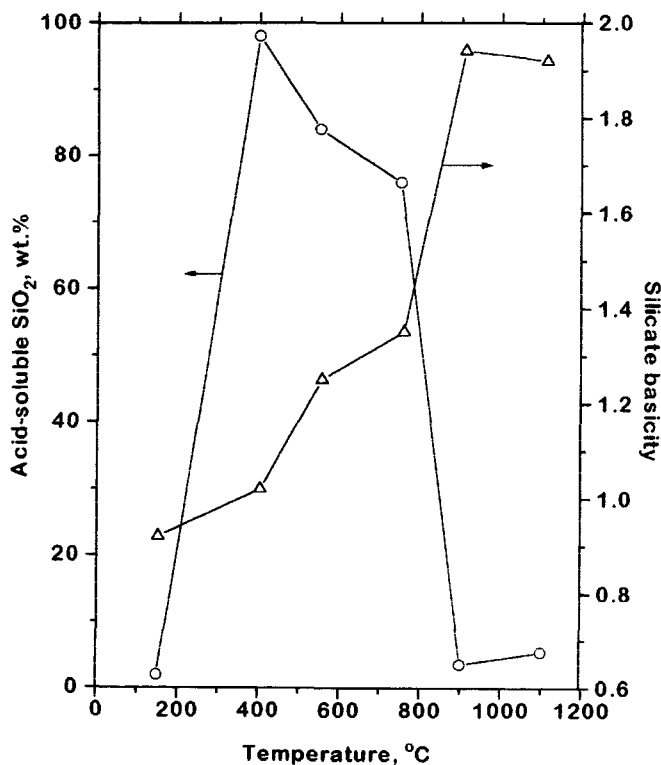
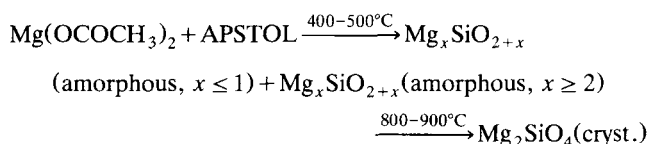


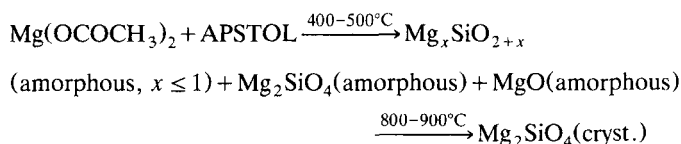
Figure 4. Percentage of acid-soluble silica (circles) and the average basicity of silicate anions (triangles) vs. temperature for the APSTOL- $\text{Mg}(\text{OCOCH}_3)_2$ dry gel heated at $5^\circ\text{C}/\text{min}$.

tional silicon (in groups R-SiO_{3/2}) does not react with molybdic acid and, therefore, cannot be detected as acid-soluble silica. The corresponding curve in Figure 4 indicates that the decomposition of the APSTOL structure with trifunctional silicon is almost complete by 400°C with the formation of rather loose amorphous silicate structures highly soluble in HCl. This solubility decreases gradually in the temperature range 400–800°C because of the partial consolidation of these structures and diminishes abruptly with the crystallization of forsterite. On the other hand, the dependence $x-T$ shows that silicate structures formed at 400°C are on the average much more polymerized ($x \approx 1.0$) than orthosilicate. The average basicity rises with further heating but arrives at the stoichiometric value $x = 2$ only with the forsterite crystallization.

Thus, the probable general scheme of the formation of forsterite from the APSTOL-acetate precursor mixture, can be written as follows



or, neglecting the possibility of the existence of high-basicity ($x > 2$) amorphous silicates



Right after 400°C, the mixture also contains magnesium in the form of residual acetate. The concentration of high-polymerized silicate fraction and amorphous magnesia must decrease on heating from 400 to 870°C. The effective absence of detectable amounts of crystalline impurities (periclase and enstatite) in the system at 1,000°C suggests that the microheterogeneity at intermediate temperatures should be on the nm rather than on the μm scale.

Conclusions

The synthetic method proposed here can be efficient for the preparation of forsterite ceramics provided that the heat treatment up to 900–1,000°C is performed to guarantee the completion of three processes: formation of the orthosilicate anion structure, crystallization of forsterite, and complete oxidation of residual carbon. Such an approach appears to be suitable for the preparation of ceramic powders and binders

as well as ceramic coatings on various substrates. In the latter case, a much softer heat treatment procedure may be used to prepare carbon-free glassy films considering relatively easy oxidizability of residual carbon in thin films. As compared with TEOS-based precursor systems, the proposed precursors have such additional advantages as the absence of organics solvents, the possibility of their storing in the form of water-soluble dry powders, and the absolute stability of their aqueous solutions.

Acknowledgment

The authors are grateful to Dr. G. Brusatin for the FTIR experiments.

Literature Cited

- Baraldi, P., "Thermal Behavior of Metal Carboxylates: III—Metal Acetates," *Spectrochimica Acta*, **38A**, 51 (1982).
- Burlitch, J. M., M. L. Beeman, B. Riley, and D. L. Kohlstedt, "Low-Temperature Syntheses of Olivine and Forsterite Facilitated by Hydrogen Peroxide," *Chem. Mater.*, **3**, 692 (1991).
- Gardner, T. J., and G. L. Messing, "Magnesium Salt Decomposition and Morphological Development during Evaporative Decomposition of Solutions," *Thermochimica Acta*, **78**, 17 (1984).
- Handke, M., and M. Urban, "IR and Raman Spectra of Alkaline Earth Metals Orthosilicates," *J. Molec. Struct.*, **79**, 353 (1982).
- Iler, R. K., *The Chemistry of Silica*, Vol. 1, Wiley, New York (1979).
- Innocenzi, P., M. O. Abdirashid, and M. Guglielmi, "Structure and Properties of Sol-Gel Coatings from Methyltriethoxysilane and Tetraethoxysilane," *J. Sol-Gel Sci. Technol.*, **3**, 47 (1994).
- Maliavski, N., E. Tchekounova, E. Martyncheva, and G. Aleksandrova, "The Complex Method to Analyze the Phase Composition of High-Polymerized Silicates," No. 11360-85, *Dep. ONITECHIM* (Tcherkassy) (1985).
- Maliavski, N., and M. Guglielmi, "Amine-Silicate Method: an Alternative Gel Method for the Synthesis of Amorphous Silicates," *Ultrastructure Processing of Advanced Ceramics*, J. D. Mackenzie and D. R. Ulrich, eds., Wiley, New York, p. 315 (1988).
- Maliavski, N., E. Tchekounova, and O. Dushkin, "Silica Fibers Obtained from Aminosilicate Solutions with a Reversible Spinnability," *J. Sol-Gel Sci. Technol.*, **2**, 503 (1994).
- Maliavski, N., O. Dushkin, E. Tchekounova, J. Markina, and G. Scarinci, "An Organic-Inorganic Silica Precursor Suitable for the Sol-Gel Synthesis in Aqueous Media," *J. Sol-Gel Sci. Technol.*, **8**, 571 (1997).
- Murakami, M., K. Izumi, T. Deguchi, A. Morita, N. Tohge, and T. Minami, "SiO₂ Coating on Stainless Steel Sheets from CH₃Si(OC₂H₅)₃," *J. Ceram. Soc. Jpn. Int. Ed.*, **97**, 86 (1989).
- Saiki, G., and T. Kanai, "Electrical Insulation Coating on Silicon Steel Sheet," *Jpn. Kokai Tokkyo Koho JP*, patent no. 60,258,477 [85,258,477] (1985).
- Wang, D., and F. R. Jones, "Surface Analytical Study of the Interaction between γ -Amino Propyl Triethoxysilane and E-Glass Surface: II. X-Ray Photoelectron Spectroscopy," *J. Mater. Sci.*, **28**, 2481 (1993).

Manuscript received Oct. 28, 1996, and revision received Apr. 28, 1997.